ARTICLE

Traditional Medicine Research 2025;37(12):23. https://doi.org/10.53388/TMR20250407002

Investigating the potential mechanisms of *Wenqing Yin* against atopic dermatitis based on network pharmacology, experimental pharmacology, and molecular docking

Yi-Xuan Li[1, 2#], **Yi Liao**[1], **Cheng-Hong Sun**[3], **Di Zhang**[1*], **Shu-Jie Tang**[1*], **Guo-Dong Sun**[4, 5*], **Guo-Dong Sun**[#*]

[1]School of Chinese Medicine, Jinan University, 601 Huangpu Avenue West, Tianhe District, Guangzhou, 510632, China
[2]Guangzhou Medical University Affiliated Traditional Chinese Medicine Hospital, No. 16 Zhuji Road, Liwan District, Guangzhou, 510130, China
[3]State Key Laboratory of Generic Manufacture Technology of Chinese Traditional Medicine, Lunan Pharmaceutical Group Co., Ltd., No. 209 Hongqi Road, Lanshan District, Linyi, 276000, China
[4]Guandgong Provincial Key Laboratory of Spine and Spinal Cord Reconstruction, The Fifth Affiliated Hospital (Heyuan Shenhe People's Hospital), Jinan University, Donghuan Road, Zijin, Heyuan 517000, China
[5]Department of Orthopedics, First Affiliated Hospital, Jinan University, 613 Huangpu Avenue West, Tianhe District,Guangzhou, 510632, China

[#]These authors contributed equally to this work and are co-first authors for this paper.
[*]**Correspondence to:**Wei Quan, Department of Pharmacy, Affiliated Hospital of Shaanxi University of Chinese Medicine, No. 6, Weiyang West Road, Xianyang712000, China. E-mail: fmmuquanwei@163.com. Ya-Jun Shi, School of Pharmacy, Shaanxi University of Chinese Medicine, No. 1, Middle Section of CenturyAvenue, Xi'an 712046, China..

Author contributions
Han SY was responsible for formal analysis, investigation, and methodology. Wang JH was responsible for conceptualization, supervision, and writing the original draft. All authors have read and agreed to the published version of the manuscript.
Competing interests
The authors declare no conflicts of interest.
Acknowledgments
We gratefully acknowledge Prof. Hojun Kim of the College of Korean Medicine, Dongguk University, for his institutional support and encouragement throughout the preparation of this Perspective. This study was supported by the National Research Foundation of Korea (2020R1F1A1074155).
Peer review information
Traditional Medicine Research thanks all anonymous reviewers for their contribution to the peer review of this paper

Abbreviations
AAA, aromatic amino acids; ALD, alcoholic liver disease; BCAA, branched-chain amino acids; CHOL, cholesterol; HF, herbal formula; HYP, hyperlipidemia; KM mice, Kunming mice; NOD, non-obese diabetic; SCFAs, short-chain fatty acids; SD rat, Sprague-Dawley rat; T1D, type 1 diabetes; T2D, type 2 diabetes; Treg, regulatory T cells.

Citation
Han SY, Wang JH. Therapeutic potential of Prevotella spp. in metabolic disorders: integrating herbal medicine and gut microbiome. Tradit Med Res. 2026;11(2):9. doi: 10.53388/TMR20250806001.

Executive editor: jinlei wang.
Received: 16 January 2025; **Revised:** 27 February 2025
Accepted: 16 May 2025; **Available online:** 17 July 2025

Abstract
Background: Wenqing Yin (WQY) is a classic prescription used to treat skin diseases like atopic dermatitis (AD) in China, and the aim of this study is to investigate the therapeutic effects and molecular mechanisms of WQY on AD. Methods: The DNFB-induced mouse models of AD were established to investigate the therapeutic effects of WQY on AD. The symptoms of AD in the ears and backs of the mice were assessed, while inflammatory factors in the ear were quantified using quantitative real-time-polymerase chain reaction (qRT-PCR), and the percentages of CD4+ and CD8+ cells in the spleen were analyzed through flow cytometry. The compounds in WQY were identified using ultra-performance liquid chromatography-tandem mass spectrometry (UPLC-MS/MS) analysis and the key targets and pathways of WQY to treat AD were predicted by network pharmacology. Subsequently, the key genes were tested and verified by qRT-PCR, and the potential active components and target proteins were verified by molecular docking.

Keywords: Wenqing Yin; atopic dermatitis; mouse model; UPLC-Orbitrap-MS/MS; network pharmacology

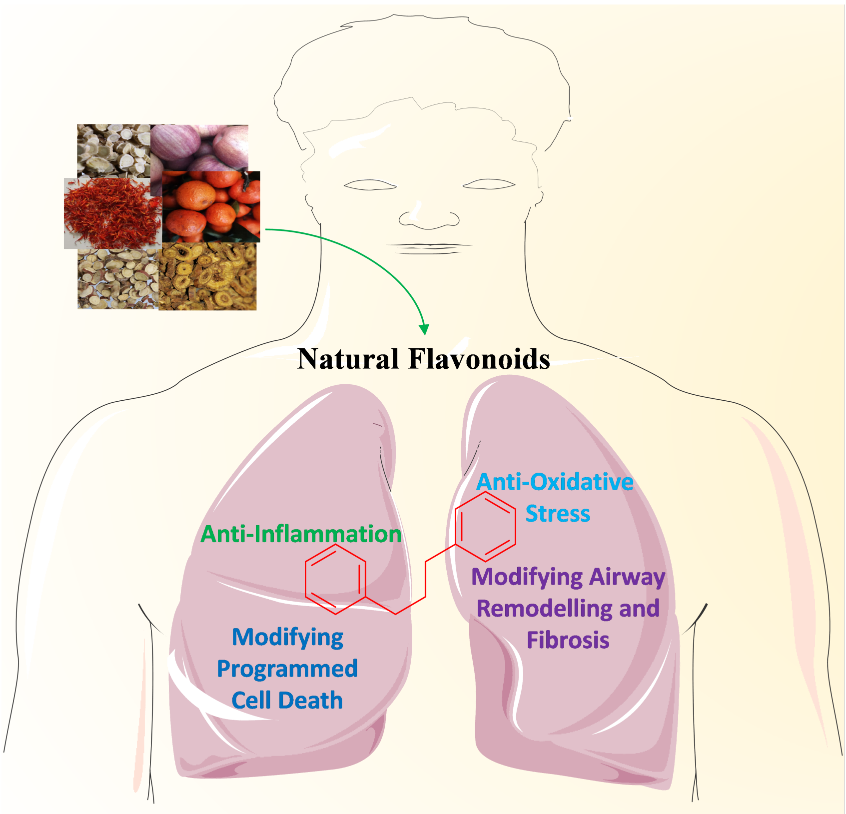

Highlights

Prevotella spp. have emerged as key modulators of host metabolism, exhibiting species-specific effects on gut barrier function, inflammation, and metabolic homeostasis. Recent evidence highlights the potential of high-fiber and herbal interventions to selectively enrich beneficial Prevotella populations. This perspective outlines an ecology-based framework that integrates herbal modulation with microbiota profiling to harness microbe-herb synergy in managing metabolic disorders.

Medical history of objective

Traditional Oriental medicine has long regarded the gastrointestinal tract as the foundation of overall health, frequently referring to the spleen–stomach axis as "the foundation of acquired constitution". Classical texts such as the Huangdi Neijing (compiled in 300–100 B.C.E.) and the Dongui Bogam (compiled in 1610 C.E. by Jun Heo) documented numerous herbal prescriptions designed to enhance digestive function and treat conditions now recognized as metabolic syndromes – characterized by fatigue, obesity, excessive thirst, and impaired digestion. Notably, many of these herbal formulas were historically used to regulate the gastrointestinal environment, "harmonize Qi movement" (keep the body's energy moving smoothly), and "eliminate internal dampness" (remove extra moisture inside the body), concepts that align with modern understandings of microbial dysbiosis, gut barrier dysfunction, and low-grade systemic inflammation. Contemporary pharmacological research has confirmed that many of these herbs and their active compounds (e.g., berberine, flavonoids, ginsenosides, etc.) can remodel the gut microbiome, modulate Prevotella abundance, and influence bile acid and short-chain fatty acids (SCFAs) pathways.

Insert A head here

This demo file is intended to serve as a "starter file". It is for preparing manuscript submission only, not for preparing camera-ready versions of manuscripts. Manuscripts will be typeset for publication by the journal, after they have been accepted.

By default, this template uses **biblatex** and adopts the Chicago referencing style. However, the journal you're submitting to may require a different reference style; specify the journal you're using with the class' **journal** option — see lines 1–7 of *sample.tex* for a list of options and instructions for selecting the journal. If you are using this template on Overleaf, Overleaf's build tool will automatically run **pdflatex** and **biber**. If you are compiling this template on your own local LaTeX installation, please execute the following commands:

1. `pdflatex sample`
2. `biber sample`
3. `pdflatex sample`
4. `pdflatex sample`

Some journals e.g. `journal=pasa`
require BibTeX. For such journals, you will need to

- delete the existing `\addbibresource{example.bib}`;
- change the existing `\printbibliography` to be `\bibliography{example}` instead.

Overleaf will run **pdflatex** and **bibtex** automatically as needed. But if you had *first* compiled using another **journal** option that adopts **biblatex**, and *then* change the **journal** option to one that adopts BibTeX, you may get some compile error messages instead. In this case you will need to do a 'Recompile from scratch'; see https://www.overleaf.com/learn/how-to/Clearing_the_cache.

On a local LaTeX installation, you would need to run these steps instead:

1. Delete `sample.aux`, `sample.bbl` if these files from a previous compile using **biber** still exist.
2. `pdflatex sample`
3. `bibtex sample`
4. `pdflatex sample`
5. `pdflatex sample`

The desired model should also provide measurable feedback describing the degree of metabolic stress experienced. To achieve this, we compared CV values with optical probing of the nicotinamide adenine dinucleotide (NADH/NAD$^+$) ratio using the NADH fluorescence signal (fNADH). Based on previous studies [ref__194007, ref__194008, ref__194009], we developed a theoretical framework summarizing current strategies for fNADH probing using photobleaching [ref__194010]. We identified a key gap: the correlation between fNADH dynamics and subsequent tissue function remains unexplored. We adapted and integrated the fNADH probing protocol into the excitation-wave optical mapping protocol. This allowed us to reveal a direct link between local changes in fNADH during metabolic stress and the delayed formation of a conduction block: the developed model made it possible to record the occurrence of a block in the long term, even in its absence, immediately after reperfusion. A comparison of CV maps and fNADH allowed us to test the entire experimental sample for a correlation between these parameters: the resistance of the NADH/NAD$^+$ ratio to photobleaching emerged as a potential prognostic parameter within each group and in the entire sample, regardless of the type of metabolic stress ($R^2 = 0.925$, $P < 0.01$). Thus, the developed model made it possible to identify and quantitatively represent the cause-and-effect chain between arrhythmogenesis and cardiac tissue remodeling, as well as to assess the capacity of cardiac tissue for controlled adaptation to metabolic stress.

Lorem ipsum dolor sit amet, consectetur adipiscing elit, sed do eiusmod tempor incididunt ut labore et dolore magna aliqua.

Lorem ipsum dolor sit amet, consectetur adipiscing elit, sed do eiusmod tempor incididunt ut labore et dolore magna aliqua. Lorem ipsum dolor sit amet, consectetur adipiscing elit, sed do eiusmod tempor incididunt ut labore et dolore magna aliqua.

Insert B head here

Subsection text here. Lorem ipsum [1] dolor sit amet, consectetur adipiscing elit, sed do eiusmod tempor incididunt ut labore et dolore magna aliqua.

Lorem ipsum dolor sit amet, consectetur [2] adipiscing elit, sed do eiusmod tempor incididunt ut labore et dolore magna aliqua. Lorem ipsum dolor sit amet, consectetur adipiscing elit, sed do eiusmod tempor incididunt ut labore et dolore magna aliqua. Lorem [3] ipsum dolor sit amet, consectetur adipiscing elit, sed do eiusmod tempor incididunt ut labore et dolore magna aliqua.

Insert C head here

Subsubsection text here. Lorem ipsum dolor sit amet, [4] consectetur adipiscing elit, sed do eiusmod tempor incididunt ut labore et dolore magna aliqua. Lorem ipsum dolor sit amet, consectetur adipiscing elit, sed do eiusmod tempor incididunt ut labore et dolore magna aliqua.

Lorem ipsum dolor sit amet, consectetur adipiscing elit, sed do eiusmod tempor incididunt ut labore et dolore magna aliqua. Lorem ipsum dolor sit amet, consectetur adipiscing elit, sed do[a] eiusmod tempor incididunt ut labore et dolore magna aliqua.

Equations

Sample equations. Lorem ipsum dolor sit amet, consectetur adipiscing elit, sed do eiusmod tempor incididunt ut labore et dolore magna aliqua. Lorem ipsum dolor sit amet, consectetur[b] adipiscing elit, sed do eiusmod tempor incididunt ut labore et dolore magna aliqua. Lorem ipsum dolor sit amet, consectetur adipiscing elit, sed do eiusmod tempor incididunt ut labore et dolore magna aliqua.

The historical use of *P. incarnata* L. dates back to the Late Archaic period in North America (approximately 8000-2000 B.C.). Archaeological findings suggest that Indigenous peoples of the pre-Columbian era cultivated mutual relationships with various plant species, and *P. incarnata* L. frequently thrived as a weedy crop in human-influenced habitats [5]. The genus *Passiflora*, established by Linnaeus, includes around 520 species within the family *Passifloraceae*. Most species are climbing plants native to Central and South America, while a few are distributed across North America, Southeast Asia, and Australia [6]. Traditionally, *P. incarnata* L. has been valued in herbal medicine across different regions. In Europe, it was primarily used to treat insomnia and anxiety, whereas in North America, it was commonly consumed as a calming tea. In Brazil, the plant served multiple

[a] A footnote/endnote
[b] Another footnote/endnote

therapeutic purposes, such as acting as an analgesic, antispasmodic, anti-asthmatic, wormicidal, and sedative agent [6–8]. It has also been employed in Iraq as a sedative and narcotic [9], and in Turkey for ailments like dysmenorrhea, epilepsy, neurosis, insomnia, and neuralgia [10]. In Poland, it has been prescribed for hysteria and neurasthenia [11], while in the United States, it has been used to alleviate diarrhoea, menstrual pain, neuralgia, burns, haemorrhoids, and sleep disorders [12]. In India, *P. incarnata* L. has been administered to individuals with opiate dependence [13].

$$\begin{aligned}\frac{\partial u(t,x)}{\partial t} &= Au(t,x)\left(1-\frac{u(t,x)}{K}\right) - B\frac{u(t-\tau,x)w(t,x)}{1+Eu(t-\tau,x)},\\ \frac{\partial w(t,x)}{\partial t} &= \delta\frac{\partial^2 w(t,x)}{\partial x^2} - Cw(t,x) + D\frac{u(t-\tau,x)w(t,x)}{1+Eu(t-\tau,x)},\end{aligned} \tag{1}$$

Lorem ipsum dolor sit amet, consectetur adipiscing elit, sed do eiusmod tempor incididunt ut labore et dolore magna aliqua. Lorem ipsum dolor sit amet, consectetur adipiscing elit, sed do eiusmod tempor incididunt ut labore et dolore magna aliqua. Lorem ipsum dolor sit amet, consectetur adipiscing elit, sed do eiusmod tempor incididunt ut labore et dolore magna aliqua.

$$\begin{aligned}\frac{dU}{dt} &= \alpha U(t)(\gamma - U(t)) - \frac{U(t-\tau)W(t)}{1+U(t-\tau)},\\ \frac{dW}{dt} &= -W(t) + \beta\frac{U(t-\tau)W(t)}{1+U(t-\tau)}.\end{aligned} \tag{2}$$

$$\begin{aligned}\left.\frac{\partial(F_1,F_2)}{\partial(c,\omega)}\right|_{(c_0,\omega_0)} &= \left|\begin{matrix}\frac{\partial F_1}{\partial c} & \frac{\partial F_1}{\partial \omega}\\ \frac{\partial F_2}{\partial c} & \frac{\partial F_2}{\partial \omega}\end{matrix}\right|_{(c_0,\omega_0)}\\ &= -4c_0 q\omega_0 - 4c_0\omega_0 p^2 = -4c_0\omega_0(q+p^2) > 0.\end{aligned}$$

$$Y_\theta^{n+1} = \sum_{w\in X(\theta)} Y^n\left(h_w^n, h_w, e_w^n\right) \tag{3}$$

$$(Vc - Vt)\times 100/Vc \tag{3}$$

Figures & Tables

The output for a single-column figure is in Figure 1. Lorem ipsum dolor sit amet, consectetur adipiscing elit, sed do eiusmod tempor incididunt ut labore et dolore magna aliqua. Lorem ipsum dolor sit amet, consectetur adipiscing elit, sed do eiusmod tempor incididunt ut labore et dolore magna aliqua. Lorem ipsum dolor sit amet, consectetur adipiscing $M_p = 0.749\times\sqrt{N_{\max}}$ elit, sed do eiusmod tempor incididunt ut labore et dolore magna aliqua.

Lorem ipsum dolor sit amet, consectetur adipiscing elit, sed do eiusmod tempor incididunt ut labore et dolore magna aliqua. Lorem ipsum dolor sit amet, consectetur adipiscing elit, sed do eiusmod tempor incididunt ut labore et dolore magna aliqua. Lorem ipsum dolor sit amet, consectetur adipiscing elit, sed do eiusmod tempor incididunt ut Figure 2 labore et dolore magna aliqua.

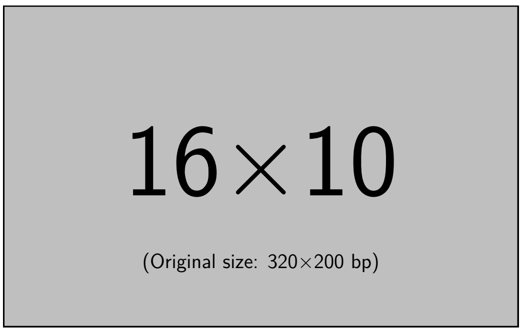

Figure 1 Insert figure caption here

See example table in Table 1.

Conclusion

The conclusion text goes here.

Acknowledgments We are grateful for the technical assistance of A. Author.

Funding Statement This research was supported by grants from the <funder-name><doi>(<award ID>); <funder-name><doi>(<award ID>).

Competing Interests A statement about any financial, professional, contractual or personal relationships or situations that could be perceived to impact the presentation of the work — or 'None' if none exist

Data Availability Statement A statement about how to access data, code and other materials allowing users to understand, verify and replicate findings — e.g. Replication data and ?? code can be found in Harvard Dataverse: `\url{https://doi.org/link}`.

Ethical Standards The research meets all ethical guidelines, Table 1 including adherence to the legal requirements of the study country.

Author Contributions Please provide an author contributions statement using the CRediT taxonomy roles as a guide `\url{https://www.casrai.org/credit.html}`. Conceptualization: A.A; A.B. Methodology: A.A; A.B. Data curation: A.C. Data visualisation: A.C. Writing original draft: A.A; A.B. All authors approved the final submitted draft.

References

1. Ethel Bayer-Santos, Clemente Aguilar-Bonavides, Silas Pessini Rodrigues, et al. Proteomic analysis of Trypanosoma cruzi secretome: characterization of two populations of extracellular vesicles and soluble proteins. *Journal of Proteome Research*. 2013;12(2):883–897. Available at: https://doi.org/10.1021/pr300948z.
2. Camila M Adade, Solange L de Castro, Maurilio J Soares. Ultrastructural localization of *Trypanosoma cruzi* lysosomes by aryl sulphatase cytochemistry. *Micron*. 2007;38(3):252–256. Available at: https://doi.org/10.1016/j.micron.2006.11.003.
3. Zheng R, Deng K, Jin H, et al. An Improved CNN-Based Pneumoconiosis Diagnosis Method on X-ray Chest Film. *Lecture Notes in Computer Science*. 2019;2019:647. Available at: https://doi.org/10.1007/978-3-030-37429-7_66.
4. Wang D, Arzhaeva Y, Devnath L, et al. Automated Pneumoconiosis Detection on Chest X-Rays Using Cascaded Learning with Real and Synthetic Radiographs. *2020 Digital Image Computing: Techniques and Applications (DICTA)*. 2020;2020:1. Available at: https://doi.org/10.1109/DICTA51227.2020.9363416.
5. Kundu R, Das R, Geem ZW, et al. Pneumonia detection in chest X-ray images using an ensemble of deep learning models. *PLOS One*. 2021;16(9):e0256630. Available at: https://doi.org/10.1371/journal.pone.0256630.
6. Yang F, Tang ZR, Chen J, et al. Pneumoconiosis computer aided diagnosis system based on X-rays and deep learning. *BMC Med Imaging*. 2021;21(1):189. Available at: https://doi.org/10.1186/s12880-021-00723-z.
7. Devnath L, Luo S, Summons P, et al. Deep Ensemble Learning for the Automatic Detection of Pneumoconiosis in Coal Worker's Chest X-ray Radiography. *JCM*. 2022;11(18):5342. Available at: https://doi.org/10.3390/jcm11185342.
8. Okumura E, Kawashita I, Ishida T. Computerized Classification of Pneumoconiosis on Digital Chest Radiography Artificial Neural Network with Three Stages. *J Digit Imaging*. 2017;30(4):413. Available at: https://doi.org/10.1007/s10278-017-9942-0.

Traditional Medicine Research 2025;37(12):23. https://doi.org/10.53388/TMR20250407002

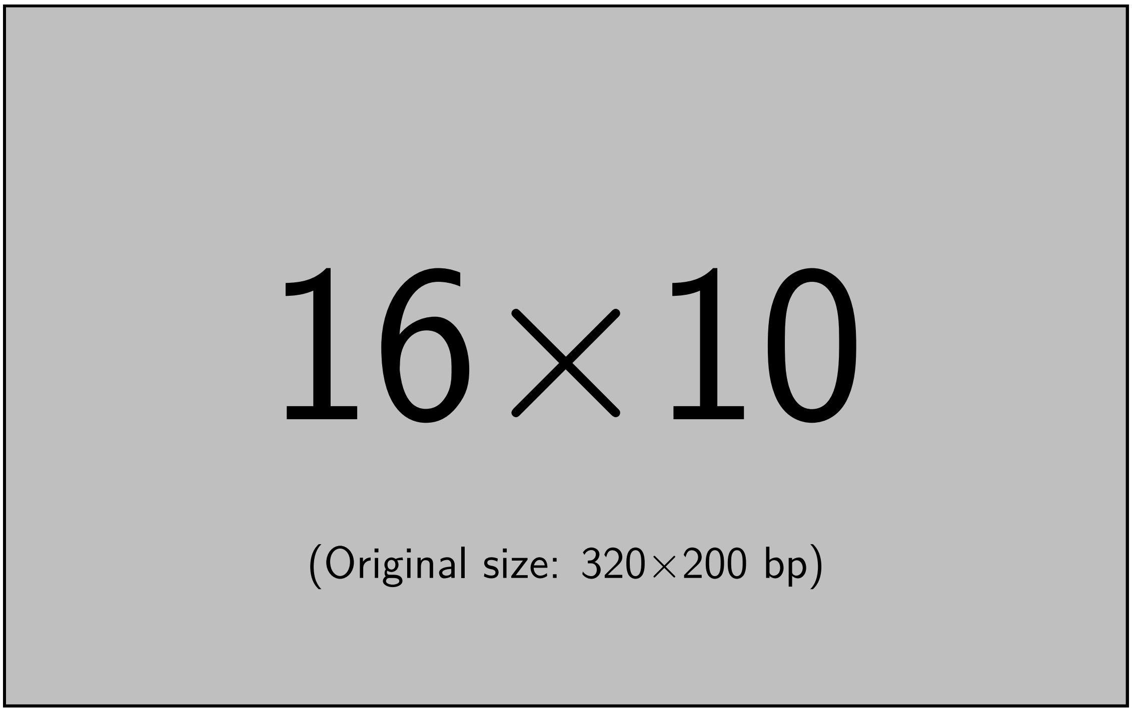

Figure 2 Insert figure caption here

Figure 3 **Transfer Learning Process for 4 Labels Profusion**

(a) depicts initialization of a DenseNet-121 model with ImageNet weights to start with a network that already has a good understanding of basic image features and Image (b) depicts the pre-trained weights act as a form of knowledge transfer from the ImageNet task to target domain of Chest X-ray profusion classification task.

Traditional Medicine Research 2025;37(12):23. https://doi.org/10.53388/TMR20250407002

frou	bbht	sadsa	fdsfds
fdsfds(n=50)		sdvfdg±SD	fesfsdfds
fdsfd	fdffds(mmol/L)	5.2±0.8	3.9-6.1
	dfse(mmHg)	120/80±5	90-140/60-90
fesfe(n=50)		fesf±SD	fesfef
fefe	fgvcbvc(mmol/L)	6.8±1.2	3.9-6.1
	sadwadwa(mmHg)	135/90±8	90-140/60-90
fweafwa			<0.05
fesfe(n=50)		fesf±SD	fesfef
fefe	fgvcbvc(mmol/L)	6.8±1.2	3.9-6.1
	sadwadwa(mmHg)	135/90±8	90-140/60-90
fweafwa			<0.05

Table 1

Cluster-ID	Number of targets	Descriptive
Cluster 1	94	Human cytomegalovirus infection
Cluster 2	11	Adenosine P1 receptors
Cluster 3	2	Muscarinic acetylcholine receptors

9. Arzhaeva Y, Wang D, Devnath L, et al. Development of Automated Diagnostic Tools for Pneumoconiosis Detection from Chest X-Ray Radiographs. *Coal Services Health and Safety Trust Project No. 20647*;192938.
10. Akgün M, Ozmen I, Ozari Yildirim E, et al. Pitfalls of using the ILO classification for silicosis compensation claims. *Occup Med*. 2022;72(6):372. Available at: https://doi.org/10.1093/occmed/kqac010.
11. JP NA, Suganuma N. Quality assurance in reading radiographs for pneumoconiosis: AIR Pneumo program. *ASEAN J Radiol*. 2020;21(1):73. Available at: https://doi.org/10.46475/aseanjr.v21i1.61.
12. DeLight N, Sachs H. Pneumoconiosis. 2023;2023.
13. International Labour Office. Guidelines for the use of the ILO International Classification of Radiographs of Pneumoconioses Revised edition 2011. 2011;2011.
14. Institute for Health Metrics and Evaluation. Findings from the global burden of disease study 2017. 2018;2018.
15. Qi XM, Luo Y, Song MY, et al. Pneumoconiosis: current status and future prospects. *Chin Med J (Engl)*. 2021;134(8):898. Available at: https://doi.org/10.1097/CM9.0000000000001461.
16. Pham QT. Chest radiography in the diagnosis of pneumoconiosis. *Int J Tuberc Lung Dis*. 2001;5(5):478.
17. International Labour Organization. ILO International Classification of Radiographs of Pneumoconioses (2023). 2023;21:February.
18. Shortliffe EH, Cimino JJ, eds. Biomedical Informatics. *Springer International Publishing*. 2021;2021. Available at: https://doi.org/10.1007/978-3-030-58721-5.
19. Alpaydin E. Introduction to Machine Learning. 4th Edition. 2020;2020.
20. LeCun Y, Bengio Y, Hinton G. Deep learning. *Nature*. 2015;521(7553):436. Available at: https://doi.org/10.1038/nature14539.
21. Deng J, Dong W, Socher R, et al. ImageNet: A large-scale hierarchical image database. *IEEE Conference on Computer Vision and Pattern Recognition*. 2009;2009:248. Available at: https://doi.org/10.1109/CVPR.2009.5206848.
22. Paszke A, Chaurasia A, Kim S, et al. ENet: A Deep Neural Network Architecture for Real-Time Semantic Segmentation. 2016;2016. Available at: https://doi.org/10.48550/ARXIV.1606.02147.
23. Sharma S, Guleria K. A Deep Learning based model for the Detection of Pneumonia from Chest X-Ray Images using VGG-16 and Neural Networks. *Proc Comput Sci*. 2023;218:357. Available at: https://doi.org/10.1016/j.procs.2023.01.018.
24. Newra N. Lung Mask Image Dataset. *kaggle*. 2022;2022.
25. Candemir S, Jaeger S, Palaniappan K, et al. Lung Segmentation in Chest Radiographs Using Anatomical Atlases With Nonrigid Registration. *IEEE Trans Med Imaging*. 2014;33(2):577. Available at: https://doi.org/10.1109/TMI.2013.2290491.
26. Jaeger S, Karargyris A, Candemir S, et al. Automatic Tuberculosis Screening Using Chest Radiographs. *IEEE Trans Med Imaging*. 2014;33(2):233. Available at: https://doi.org/10.1109/TMI.2013.2284099.
27. Ronneberger O, Fischer P, Brox T. U-Net: Convolutional Networks for Biomedical Image Segmentation. *Lecture Notes in Computer Science*. 2015;2015:234. Available at: https://doi.org/10.1007/978-3-319-24574-4_28.
28. Long J, Shelhamer E, Darrell T. Fully convolutional networks for semantic segmentation. *IEEE Trans Pattern Anal Mach Intell*;201. Available at: https://doi.org/10.1109/CVPR.2015.7298965.
29. He K, Gkioxari G, Dollar P, et al. Mask R-CNN. *2017 IEEE International Conference on Computer Vision (ICCV)*. 2017;2017:2980. Available at: https://doi.org/10.1109/ICCV.2017.322.

30. Chen L-C, Papandreou G, Kokkinos I, et al. DeepLab: Semantic Image Segmentation with Deep Convolutional Nets, Atrous Convolution, and Fully Connected CRFs. *IEEE Trans Pattern Anal Mach Intell*. 2018;40(4):834. Available at: https://doi.org/10.1109/TPAMI.2017.2699184.
31. Romero M, Interian Y, Solberg T, et al. Targeted transfer learning to improve performance in small medical physics datasets. *Med Phys*. 2020;47(12):6246. Available at: https://doi.org/10.1002/mp.14507.
32. He K, Zhang X, Ren S, et al. Deep Residual Learning for Image Recognition. *2016 IEEE Conference on Computer Vision and Pattern Recognition (CVPR)*. 2016;2016:770. Available at: https://doi.org/10.1109/CVPR.2016.90.
33. Huang G, Liu Z, van der Maaten L, et al. Densely Connected Convolutional Networks. 2016;2016. Available at: https://doi.org/10.48550/ARXIV.1608.06993.
34. Simonyan K, Zisserman A. Very Deep Convolutional Networks for Large-Scale Visual Recognition. *International Conference on Learning Representations*. 2015;2015. Available at: https://doi.org/10.48550/arXiv.1409.1556.
35. Szegedy C, Wei Liu, Yangqing Jia, et al. Going deeper with convolutions. *2015 IEEE Conference on Computer Vision and Pattern Recognition (CVPR)*. 2015;2015:1. Available at: https://doi.org/10.1109/CVPR.2015.7298594.
36. Howard AG, Zhu M, Chen B, et al. MobileNets: Efficient Convolutional Neural Networks for Mobile Vision Applications. 2017;2017. Available at: https://doi.org/10.48550/ARXIV.1704.04861.
37. Rajpurkar P, Irvin J, Zhu K, et al. CheXNet: Radiologist-Level Pneumonia Detection on Chest X-Rays with Deep Learning. 2017;2017. Available at: https://doi.org/10.48550/ARXIV.1711.05225.
38. Jagoe JR, Paton KA. Measurement of Pneumoconiosis by Computer. *IEEE Trans Comput*. 1976;1976. Available at: https://doi.org/10.1109/TC.1976.5009212.
39. Kobatake H, Oh'ishi K, Miyamichi J. Automatic diagnosis of pneumoconiosis by texture analysis of chest X-ray images. *IEEE International Conference on Acoustics, Speech, and Signal Processing*. 1987;1987:610. Available at: https://doi.org/10.1109/ICASSP.1987.1169720.
40. Ledley RS, Huang HK, Rotolo LS. A texture analysis method in classification of coal workers' pneumoconiosis. *Comput Biol Med*. 1975;5(1–2):53. Available at: https://doi.org/10.1016/0010-4825(75)90018-9.
41. Murray V, Pattichis MS, Davis H, et al. Multiscale AM-FM analysis of pneumoconiosis x-ray images. *2009 16th IEEE International Conference on Image Processing (ICIP)*. 2009;2009:4201. Available at: https://doi.org/10.1109/ICIP.2009.5414522.
42. Cai CX, Zhu BY, Chen H. Computer-Aided Diagnosis for Pneumoconiosis Based on Texture Analysis on Digital Chest Radiographs. *Appl Mech Mater*. 2012;241. Available at: https://doi.org/10.4028/www.scientific.net/AMM.241-244.244.
43. Yu P, Xu H, Zhu Y, et al. An Automatic Computer-Aided Detection Scheme for Pneumoconiosis on Digital Chest Radiographs. *J Digit Imaging*. 2010;24(3):382. Available at: https://doi.org/10.1007/s10278-010-9276-7.
44. Pattichis MS, Pattichis CS, Christodoulou CI, et al. A screening system for the assessment of opacity profusion in chest radiographs of miners with pneumoconiosis. *Proceedings Fifth IEEE Southwest Symposium on Image Analysis and Interpretation*. 2002;2002:130. Available at: https://doi.org/10.1109/IAI.2002.999904.
45. Soliz P, Pattichis MS, Ramachandran J, et al. Computer-assisted diagnosis of chest radiographs for pneumoconioses. *SPIE Proceedings*. 2001;4322:667. Available at: https://doi.org/10.1117/12.431143.
46. Zhang L, Rong R, Li Q, et al. A deep learning-based model for screening and staging pneumoconiosis. *Sci Rep*. 2021;11(1):2201. Available at: https://doi.org/10.1038/s41598-020-77924-z.
47. Devnath L, Luo S, Summons P, et al. Automated detection of pneumoconiosis with multilevel deep features learned from chest X-Ray radiographs. *Comput Biol Med*. 2021;129:104125. Available at: https://doi.org/10.1016/j.compbiomed.2020.104125.
48. Devnath L, Luo S, Summons P, et al. Performance Comparison of Deep Learning Models for Black Lung Detection on Chest X-ray Radiographs. *Proceedings of the 3rd International Conference on Software Engineering and Information Management January*. 2020;2020:150. Available at: https://doi.org/10.1145/3378936.3378968.
49. Ehab W, Huang L, Li Y. UNet and Variants for Medical Image Segmentation. *Int J Network Dyn Intell*. 2024;3(2):100009. Available at: https://doi.org/10.53941/ijndi.2024.100009.